Palaeoentomology 005 (6): 606–622
https://www.mapress.com/j/pe/

Article

ISSN 2624-2826 (print edition)
PALAEOENTOMOLOGY
ISSN 2624-2834 (online edition)

https://doi.org/10.11646/palaeoentomology.5.6.10
http://zoobank.org/urn:lsid:zoobank.org:pub:F39F6131-9DFD-443F-807E-4B851C4A8ABA

A new species of Trichopolydesmidae (Myriapoda, Diplopoda, Polydesmida) from the mid-Cretaceous Burmese amber

YI-TONG SU, CHEN-YANG CAI & DI-YING HUANG*
State Key Laboratory of Palaeobiology and Stratigraphy, Center for Excellence in Life and Paleoenvironment, Nanjing Institute of Geology and Palaeontology, Chinese Academy of Sciences, Nanjing 210008, China
ytsu@nigpas.ac.cn; https://orcid.org/0000-0003-0547-0792
cycai@nigpas.ac.cn; https://orcid.org/0000-0002-9283-8323
dyhuang@nigpas.ac.cn; https://orcid.org/0000-0002-5637-4867
**Corresponding author*

Abstract

A new species of the 'flat-backed' millipede family Trichopolydesmidae, *Monstrodesmus grimaldii* **sp. nov.**, is described from the mid-Cretaceous Burmese amber. Detailed morphological characters are provided on the basis of three well-preserved adults (two males and one female), one male juvenile, and seven additional specimens, using confocal laser scanning microscopy (CLSM) and microcomputer tomography (μCT) with computer-aided 3D-reconstructions. The new species can be placed most likely in the extant genus *Monstrodesmus* by presenting great similarities to living species.

Keywords: Cretaceous, Myanmar, millipede, Diplopoda, Trichopolydesmidae

Introduction

Trichopolydesmidae is a large, predominantly Northern Hemisphere-distributed millipede family, belonging to the superfamily Trichopolydesmoidea in the order Polydesmida, with approximately 75 genera and 140 species (Enghoff *et al.*, 2015). No fossil trichopolydesmid has been report to date. Trichopolydesmids are characterised mainly by the small body size (usually less than 10 mm), polydesmoid body form, alveolate tegument, generally normal ozopore formula, subglobose gonopod coxae, and usually cephalad directed gonopod telopodites (Golovatch *et al.*, 2014, Enghoff *et al.*, 2015). *Monstrodesmus* Golovatch *et al.*, 2014 is a unique trichopolydesmid genus containing only one living species from southern Vietnam. It differs from other genera by tripartite gonopod telopodites with a "monstrously long" flagelliform branch (Golovatch *et al.*, 2014).

Burmese amber from Hukawng Valley in Kachin State contains diverse groups of protists, fungi, plants, invertebrates, and vertebrates (Ross, 2019). An overview of the amber deposit and its geological settings was made by Zherikhin & Ross (2000), Grimaldi *et al.* (2002), Cruickshank & Ko (2003), and Ross *et al.* (2010). The fossil record of Myriapoda is rare, but they are abundant in the mid-Cretaceous Burmese amber, especially diplopods. To date, a total of eight genera and ten species of Myriapoda have been formally described from Burmese amber. Among them, six genera and eight species of Diplopoda are documented (Wesener & Moritz, 2018, Ross, 2019, 2021).

Here, we describe a new species of Trichopolydesmidae from the mid-Cretaceous Burmese amber based on 11 individuals. The new species can be placed in the extant genus *Monstrodesmus* Golovatch *et al.*, 2014.

Material and methods

Our research is based on 11 newly discovered specimens (three males, six females and two sex-undetermined specimens) entombed in mid-Cretaceous Burmese amber, which originated from a locality near Noije Bum (26°20′N, 96°36′E), Hukawng Valley, Kachin State, northern Myanmar, with an age close to the Albian-Cenomanian boundary (Shi *et al.*, 2012; Mao *et al.*, 2018). All specimens are deposited in the Nanjing Institute of Geology and Palaeontology, Chinese Academy of Sciences, Nanjing, China.

The amber pieces containing the inclusions were cut and shaped manually with handheld engraving tool and razor blade, and polished using emery papers of different grit sizes, rare earth polishing powder, and diatomite

 Submitted: 5 Dec. 2022; accepted by D. Azar: 14 Dec. 2022; published: 23 Dec. 2022

mud (Azar *et al.*, 2003). Observations were made and photographs taken using a Zeiss Axio Zoom V16 stereo microscope and a Zeiss Axio Imager 2 light microscope with a digital camera attached. Widefield fluorescence images (green background) were captured with a Zeiss Axio Imager 2 light microscope combined with a fluorescence imaging system. Confocal images (cyan background) were obtained with a Zeiss LSM710 confocal laser scanning microscope with 5× and 10× objectives, using the 488 nm Argon laser excitation line (Fu *et al.*, 2021). The holotype was scanned using Zeiss Xradia 520 versa at the micro-CT laboratory of the Nanjing Institute of Geology and Palaeontology, Chinese Academy of Sciences in Nanjing, China. A CCD-based 4× objective was used, which provides isotropic voxel sizes of 2.424 μm (Fig. 14A–C) and 0.8813 μm (Fig. 14D, E) with the geometric magnification. The acceleration voltage for the X-ray source set at 50 kV (Fig. 14A–C) and 60 kV (Fig. 14D, E). To improve signal-to-noise ratio, 2604 (Fig. 14A–C) and 3201 (Fig. 14D, E) projections through 360° were collected, and the exposure time for each projection set at 1.5 s (Fig. 14A–C) and 5 s (Fig. 14D, E). The tomographic data were analysed using VGStudio MAX 3.0 (silver-colored reconstructions).

Classification and nomenclature of characters are based on Golovatch *et al.* (2014), Enghoff *et al.* (2015), and Siewald & Spelda (2021).

Systematic palaeontology

Class Diplopoda de Blainville *in* Gervais, 1844
Subclass Helminthomorpha Pocock, 1887
Order Polydesmida Leach, 1815
Suborder Polydesmidea Pocock, 1887
Superfamily Trichopolydesmoidea Verhoeff, 1910
Genus *Monstrodesmus* Golovatch, Geoffroy & VandenSpiegel, 2014

Type species. *Monstrodesmus flagellifer* Golovatch, Geoffroy & VandenSpiegel, 2014

***Monstrodesmus grimaldii* sp. nov.**

Materials. Holotype: NIGP175093, a well-preserved adult male (Figs 1–4, 11A, C, E, F, 12A–C, E, F, 14). Paratypes: NIGP175094–NIGP175096, one well-preserved adult male (Figs 5–6, 11B, D, 12D), one well-preserved adult female (Figs 7–8, 13A–D), one moderately preserved juvenile with 18 body-rings (Figs 9–10, 13D, E). Additional specimens: 5 females and 2 sex unknown.

Etymology. The specific epithet is given in honor of Dr David A. Grimaldi, a world authority on fossil insects and their evolution.

Diagnosis. Differs from *Monstrodesmus flagellifer* by: 20 body rings, alveolate tegument texture well-developed, body setae inserted on strongly bulged knobs, numerous averagely arranged setae on dorsal surface and margins of collum, pleurosternal carinae present, and flagelliform branch of gonopods with spines or palps along inner sides.

Locality and horizon. Noije Bum near Tanai, Hukawng Valley, Kachin State of northern Myanmar; upper Albian to lower Cenomanian (mid-Cretaceous).

Description. Body length 4.9–5.8 mm, width of mid-body metazonites 0.52–0.65 mm, 20 body rings in adult (including collum and telson). No distinct body size difference between male and female (Figs 1A, B, 5A, B, 7A, B, 9A, B).

Head densely setose except labral area, cranium normal and convex, without apical modification, (Figs 1D, E, 2D, 3E, 6C, 7D, F, 8A, B, 10C, 11A, 13A, E). Ommatidia absent. Antennae short, reaching behind collum if stretched dorsally, moderately clavate and setose; length of antennomeres 6>2>3>4≈5>1≈7, antennomere 6 slightly wider than others (Figs 1D, 2D, F, 3E, 5C, E, G, 6C, 9D, H, 10C, 11A, 13E); antennomeres 5 and 6 each with a distodorsal group of bacilliform sensilla (Figs 11B, 13A, E); isthmus between antennae about 1.5× diameter of antennal socket. Gnathochilarium broad, without visible setae (Figs 2F, 3F, 14B).

Collum large, suboval shaped, with well-developed *ca.* 60 large bacilliform setae arranged averagely on dorsal surface and along dorsal margin (Figs 1E, 2C, 3D, 7D, E, 8B, 9C, G, 14C); insertion point of setae strongly bulged to conically shaped knobs. Each following metaterga with similar setae arranged in 3 transverse rows and inserted on strong conic knobs; each row with 12–18 regularly arranged setae (Figs 2E, 4A, C, 5D, F, 6A, E, 7C, 10D, 11C, D, F). Tegument deeply alveolate. Stricture between pro- and metazonite rather wide and shallow, deeply alveolate similar to pro- and metazonite (Figs 4B, 6F, 8C, 11E, 13B, F). Paraterga moderately to weakly developed, deeply quadripartite to knobs (without ozopores attached) or obviously large lobules (with ozopores attached) laterally, with 1 bacilliform seta on each apex of knob and 2 on lobule (Figs 4A, 6E, 11C, D, 13F). Pore formula normal: 5, 7, 9, 10, 12, 13, 15–19; ozopores located closer to lateral than to caudal margin of paraterga (Figs 4A, E, 5D, 6A, E, 8D, 10D, 11C, D, 12E, 13C, F). Sterna rather broad, moderately alveolate. Legs short, sparsely setose; femur, postfemur and tibia slightly incrassate (Figs 3C, 4F, 5C, E, H, 12F); tarsus long and slender, sphaerotrichomes absent; claw simple, slightly curved. Coxae 2 with very short, cylindrical gonapophyses (Figs 3E, 11A, 12B). Pleurosternal carinae present laterally near sterna between coxae (Figs 6D, 12D, 14A).

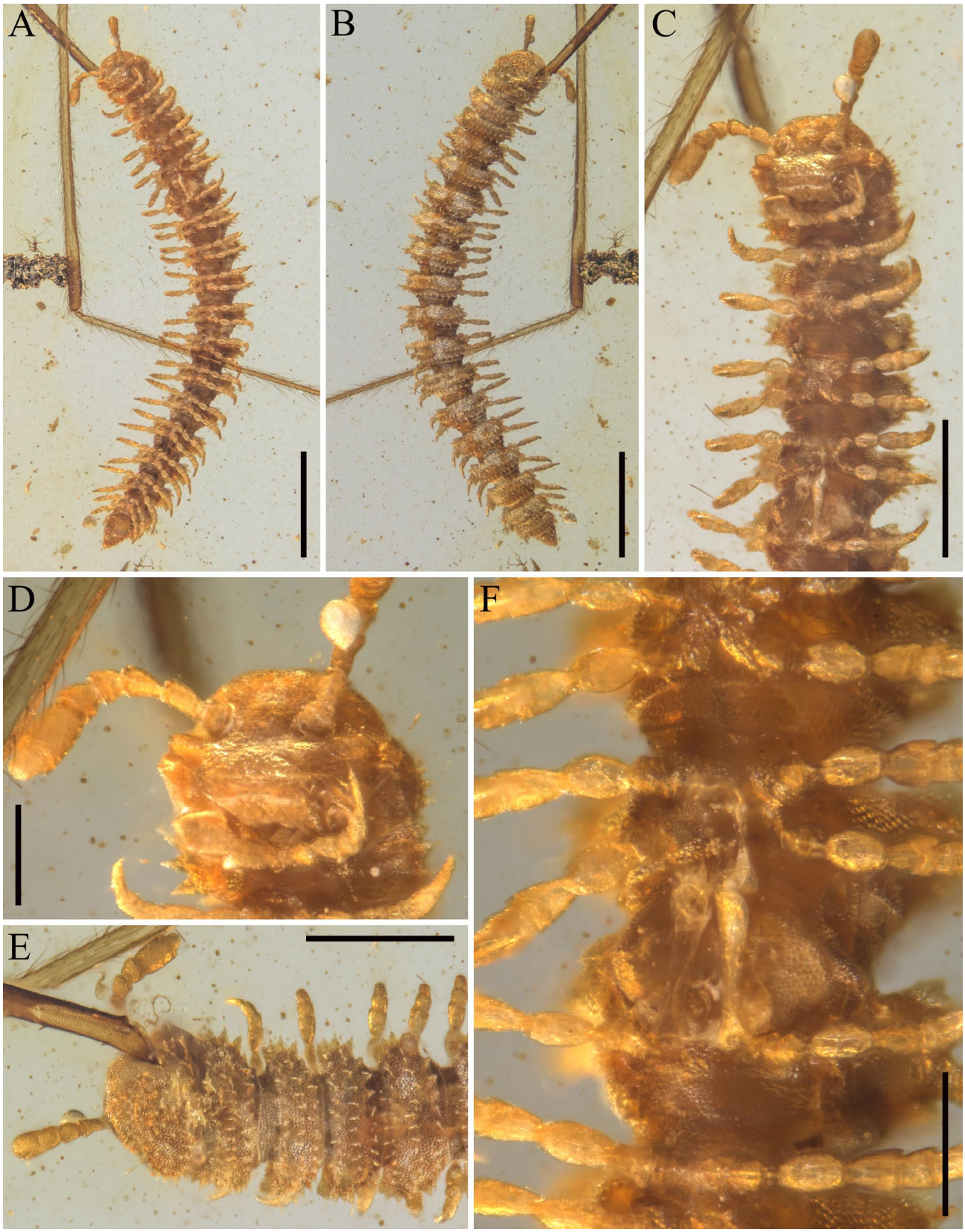

FIGURE 1. Adult male of *Monstrodesmus grimaldii* **sp. nov.**, holotype (NIGP175093). **A**, Dorsal view. **B**, Ventral view. **C**, Ventral view of the anterior body part. **D**, Ventral view of head. **E**, Dorsal view of the anterior body part. **F**, Ventral view of gonopods. Scale bars = 1 mm in **A** and **B**, 0.5 mm in **C**, 0.2 mm in **D**–**F**.

Epiproct short, conical, truncate, directed caudoventrally, with a group of 4 setiform spinnerets on tip; hypoproct subtrapeziform, caudal 1+1 setigerous papillae well-developed and separated (Figs 2A, B, 3A, B, 4E, F, 6B, 7F, G, 8D–F, 9E, F, 10A, B, E, F, 12E, F, 13C, D).

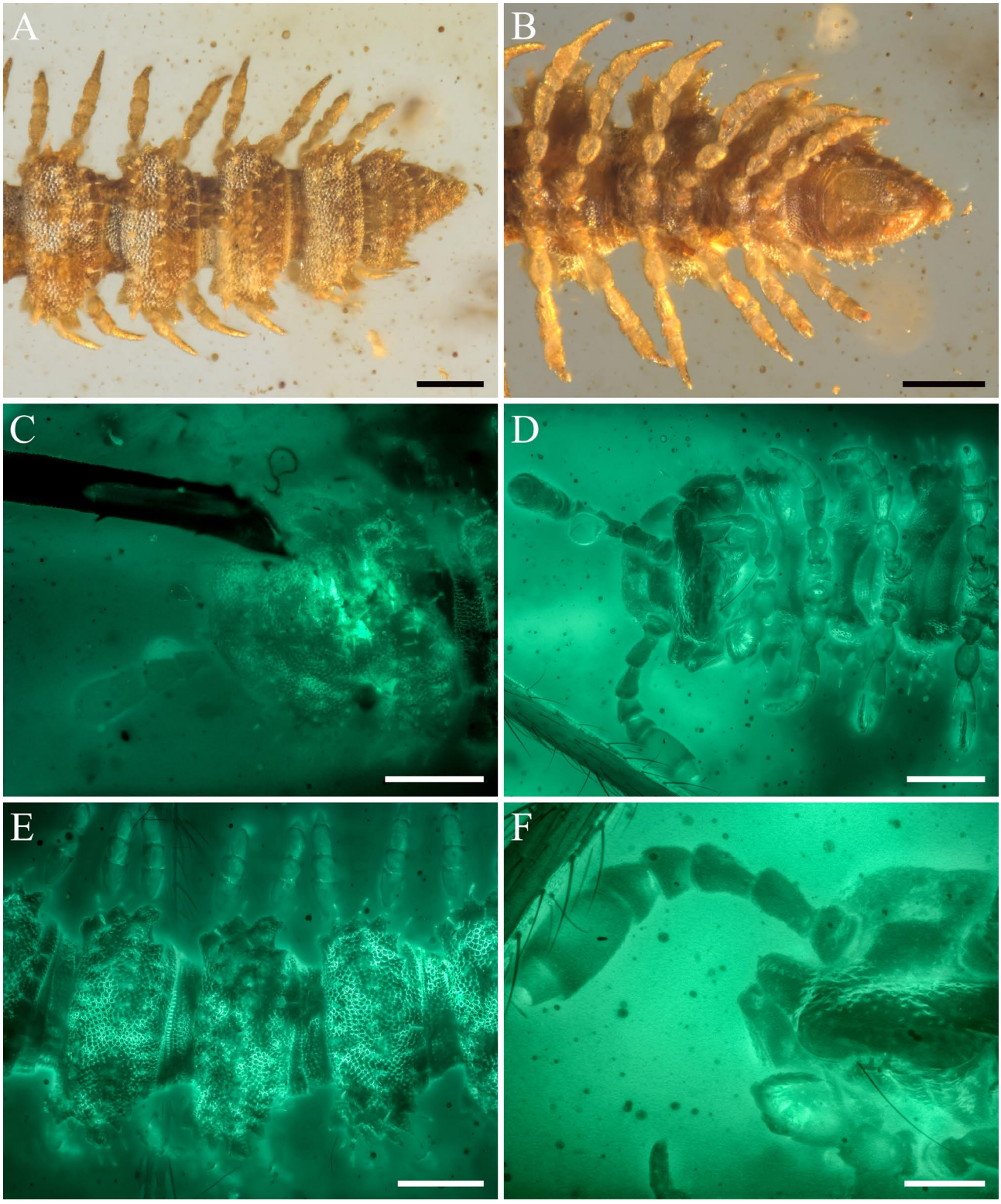

FIGURE 2. Adult male of *Monstrodesmus grimaldii* **sp. nov.**, holotype (NIGP175093). **C**–**F** under green fluorescence. **A**, Dorsal view of the posterior body part. **B**, Ventral view of the posterior body part. **C**, Dorsal view of head, collum, 2nd tergite, **D**, Ventral view of head and the anterior body part. **E**, Dorsal view of the 9th to 11th body-rings. **F**, Detail structures of head and right antenna. Scale bars = 0.2 mm.

Gonopods modified from leg pair 7 only (Figs 1C, 5C, E, 14A). Gonopod aperture with large sub-oval shape opening; coxae large and subglobose, firmly attached to edges of aperture, with alveolate texture and 2 setae. Telopodites well exposed, straight and elongate, lying appressed to venter, parallel to main body axis and directed forward (Figs 1F, 4D, 5H, 6D, 12A, D, 14D). Seminal groove not observable, making solenomere and exomere

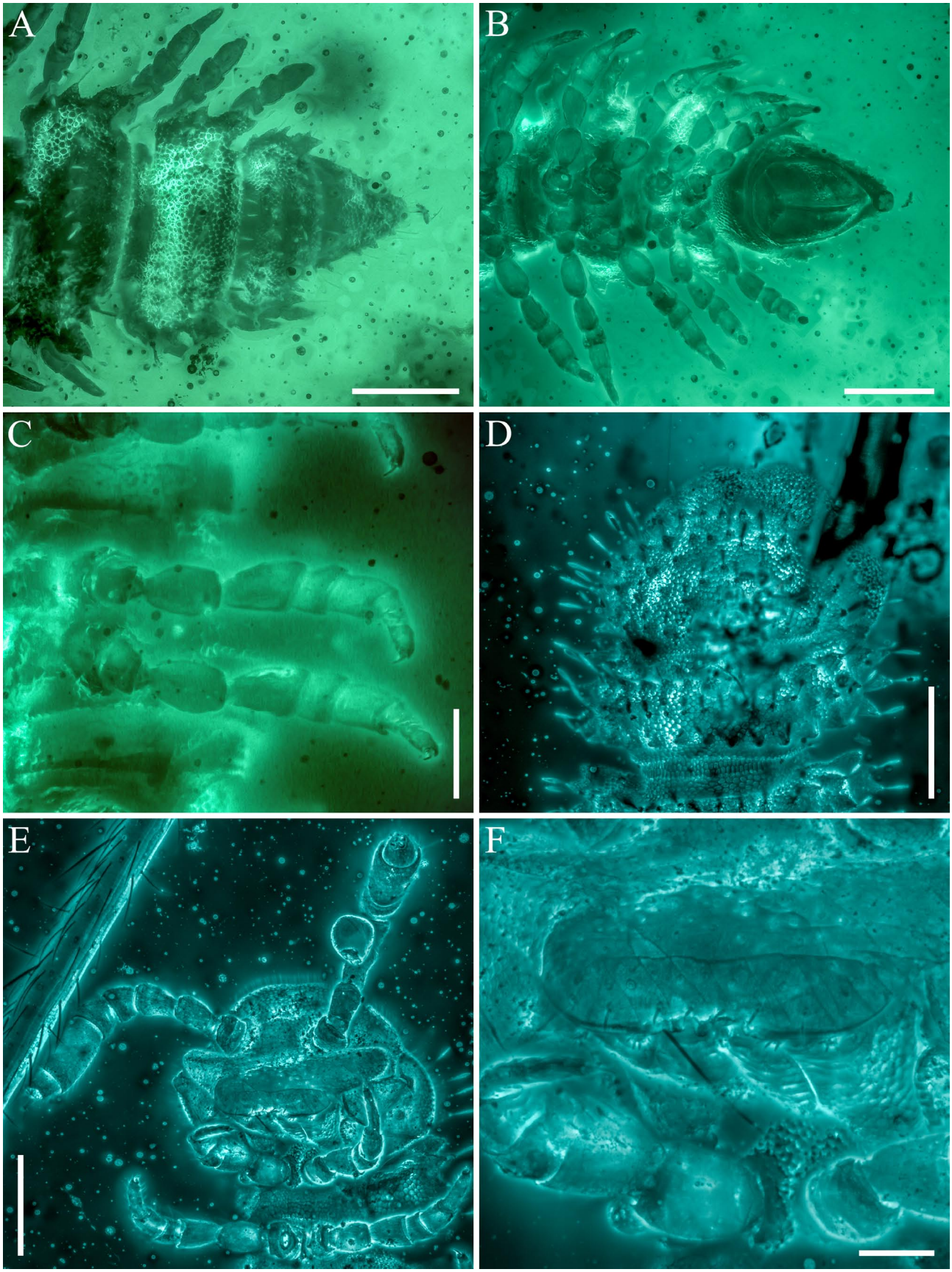

FIGURE 3. Adult male of *Monstrodesmus grimaldii* **sp. nov.**, holotype (NIGP175093). **A–C** under green fluorescence, **D–F** under CLSM. **A**, Dorsal view of the posterior body part. **B**, Ventral view of the posterior body part. **C**, Ventral view of the 22th, 23th right legs. **D**, Dorsal view of head. **E**, Ventral view of head. **F**, Detail structures of gnathochilarium. Scale bars = 200 μm in **A**, **B**, **D** and **E**, 100 μm in **C**, 50 μm in **F**.

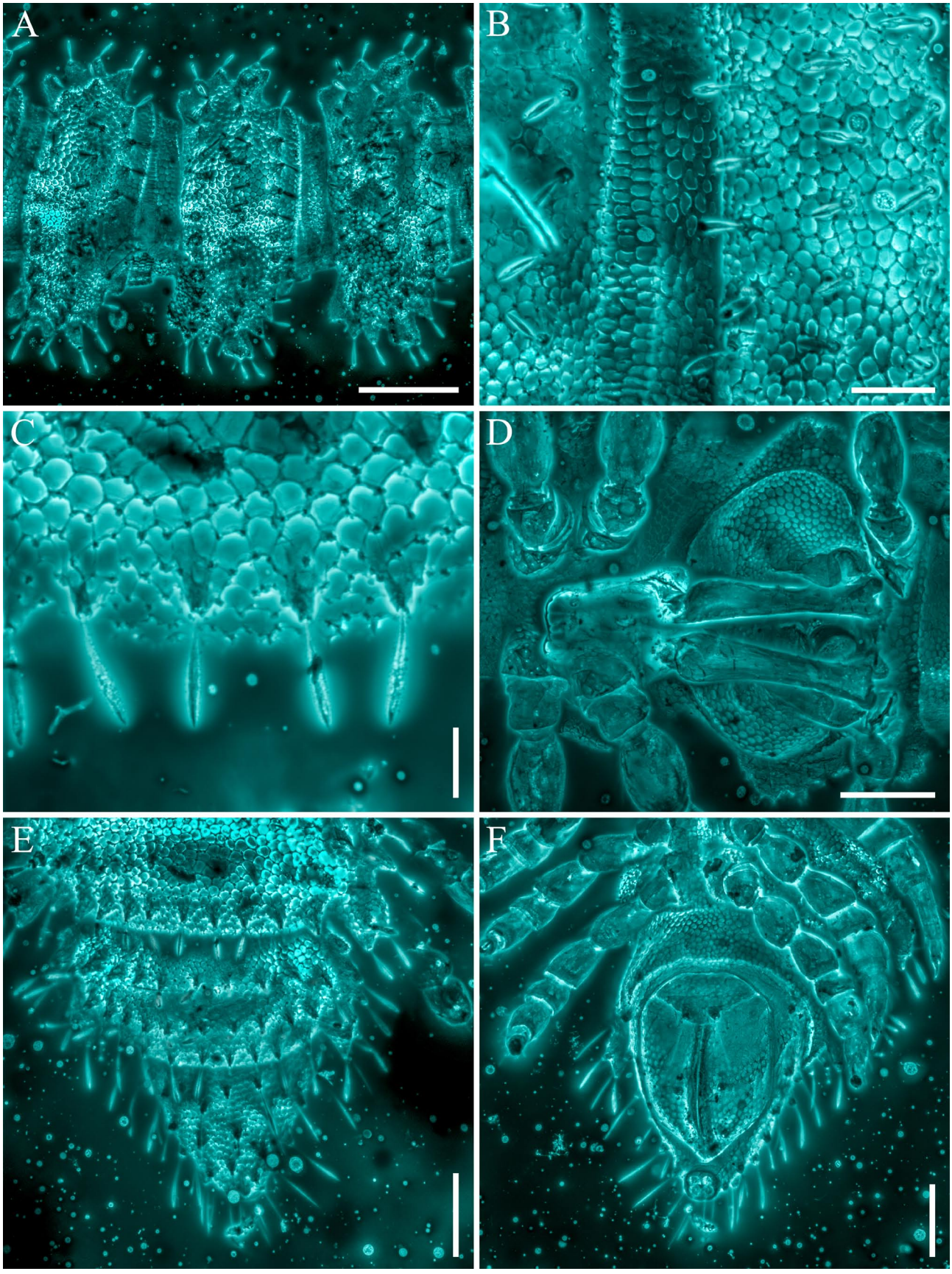

FIGURE 4. Adult male of *Monstrodesmus grimaldii* **sp. nov.**, holotype (NIGP175093), detail structures under CLSM. **A**, Dorsal view of the 8th to 10th body-rings. **B**, Detailed structures of the 2nd, 3rd tergites. **C**, Setigerous knobs on the 18th metaterga. **D**, Ventral view of gonopods. **E**, Dorsal view of the posterior body part. **F**, Detailed structures of the telson. Scale bars = 200 μm in **A**, 50 μm in **B**, 10 μm in **C**, 100 μm in **D**–**F**.

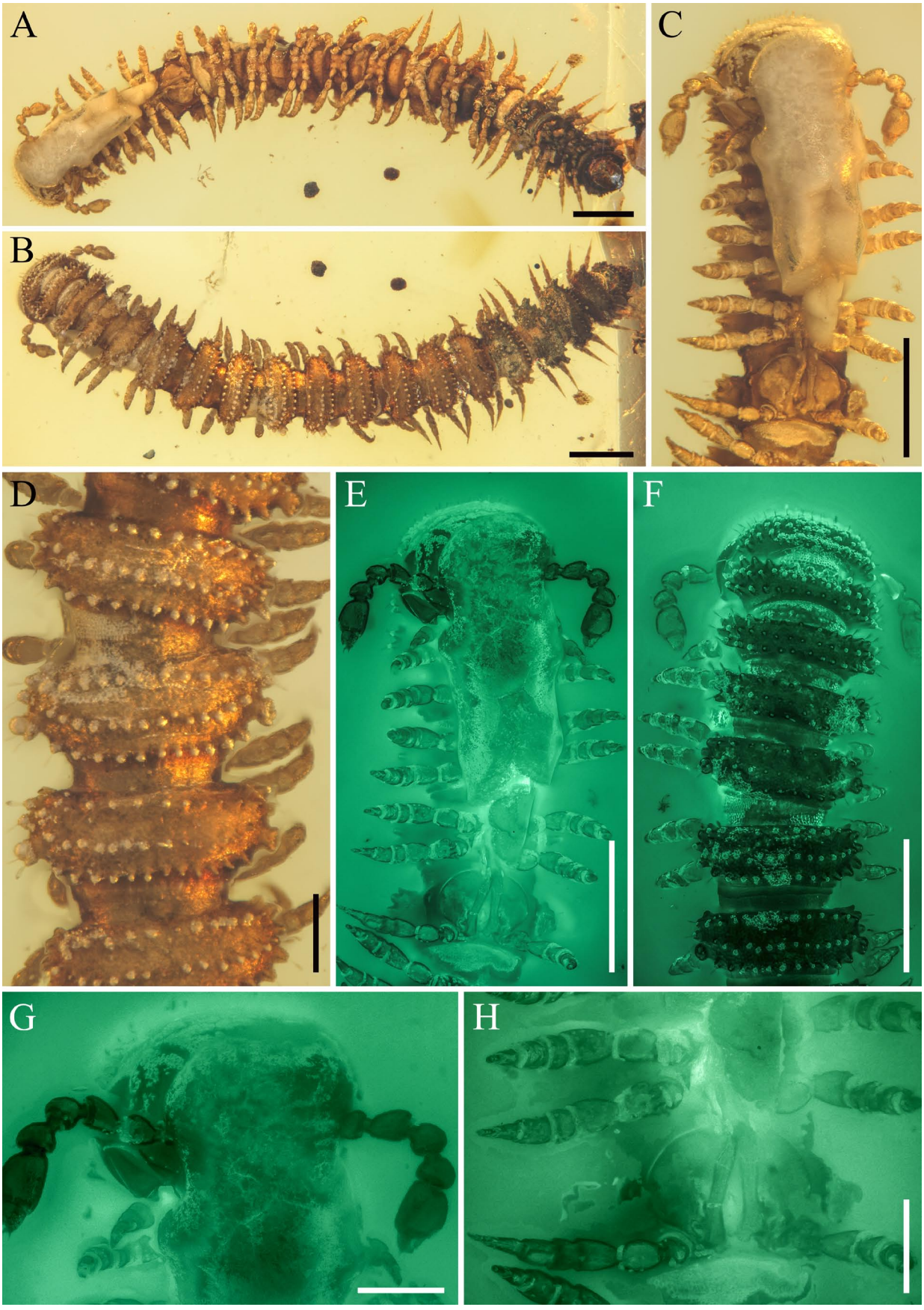

FIGURE 5. Adult male of *Monstrodesmus grimaldii* **sp. nov.**, paratype (NIGP175094). **A**, Ventral view. **B**, Dorsal view. **C**, **E**, Ventral view of the anterior body part. **D**, Dorsal view of the 6th to 9th body-rings. **F**, Dorsal view of the anterior body part. **G**, Detail structures of head and antennae. **H**, Ventral view of gonopods. Scale bars = 0.5 mm in **A**, **B**, **E** and **F**, 0.2 mm in **C**, **D**, **G** and **H**.

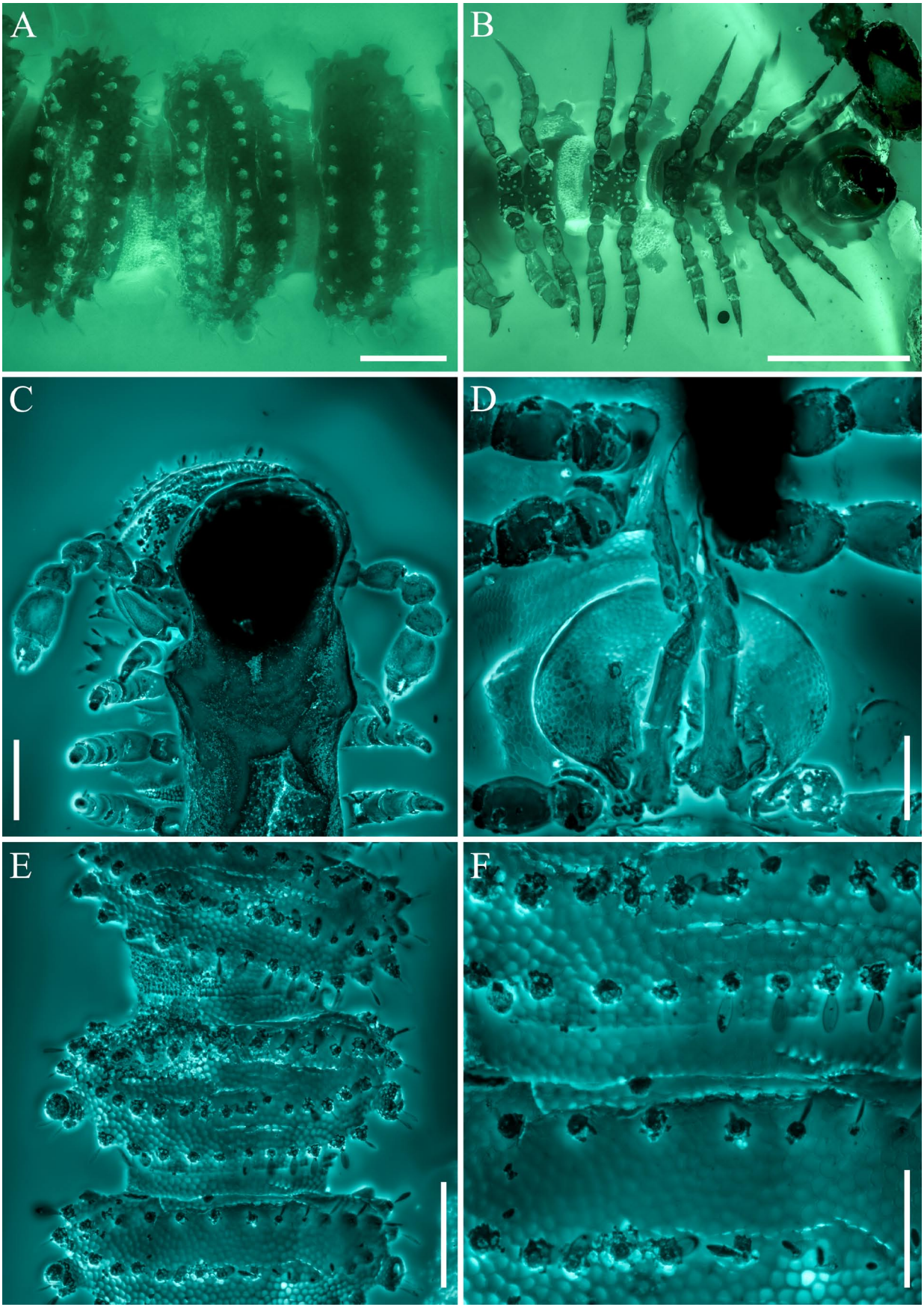

FIGURE 6. Detail structures of *Monstrodesmus grimaldii* **sp. nov.**, paratype (NIGP175094). **A**–**C** under green fluorescence, **D**–**F** under CLSM. **A**, Dorsal view of the 8th to 10th body-rings. **B**, Ventral view of the posterior body part. **C**, Ventral view of head. **D**, Ventral view of gonopods. **E**, Detail structures of the 8th to 10th body-rings. **F**, Detail structures of the 9th, 10th tergites. Scale bars = 0.2 mm in **A**, **C** and **E**, 0.5 mm in **B**, 0.1 mm in **D** and **F**.

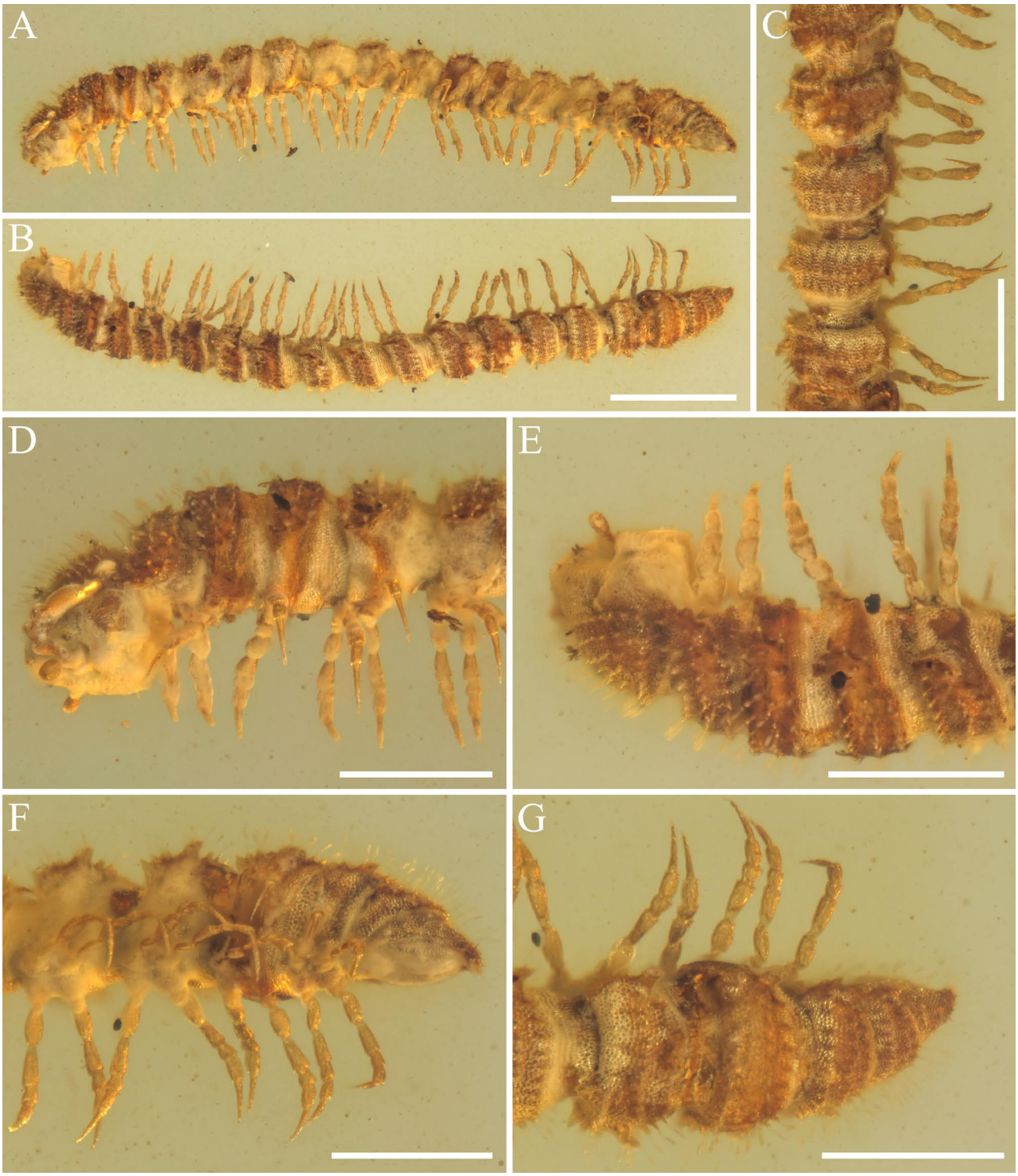

FIGURE 7. Adult female of *Monstrodesmus grimaldii* **sp. nov.**, paratype (NIGP175095). **A**, Ventrolateral view. **B**, Dorsolateral view. **C**, Dorsolateral view of the 3th to 6th body-rings. **D**, Ventrolateral view of the anterior body part. **E**, **G**, Dorsolateral view of the anterior body part. **F**, Ventrolateral view of the posterior body part. Scale bars = 1 mm in **A** and **B**, 0.5 mm in others.

indistinguishable; the simple branch close to venter may referring to solenomere according to its shape and position (Figs 12C, 14E, F). Distal part of telopodites bent dorsally, with large oval-shaped structures of unknown details (Fig. 14D–F). Flagelliform branch extreme thin and long, with delicately arranged spines or palps along the inner side (Figs 4D, 6D, 12B, D).

Discussion

The new species described here can be placed in the family Trichopolydesmidae and hypothetically in the genus *Monstrodesmus* based on the following features: body size small (< 10 mm); tegument alveolate; metaterga with 3 rows of bacilliform setae inserted on knobs; pore

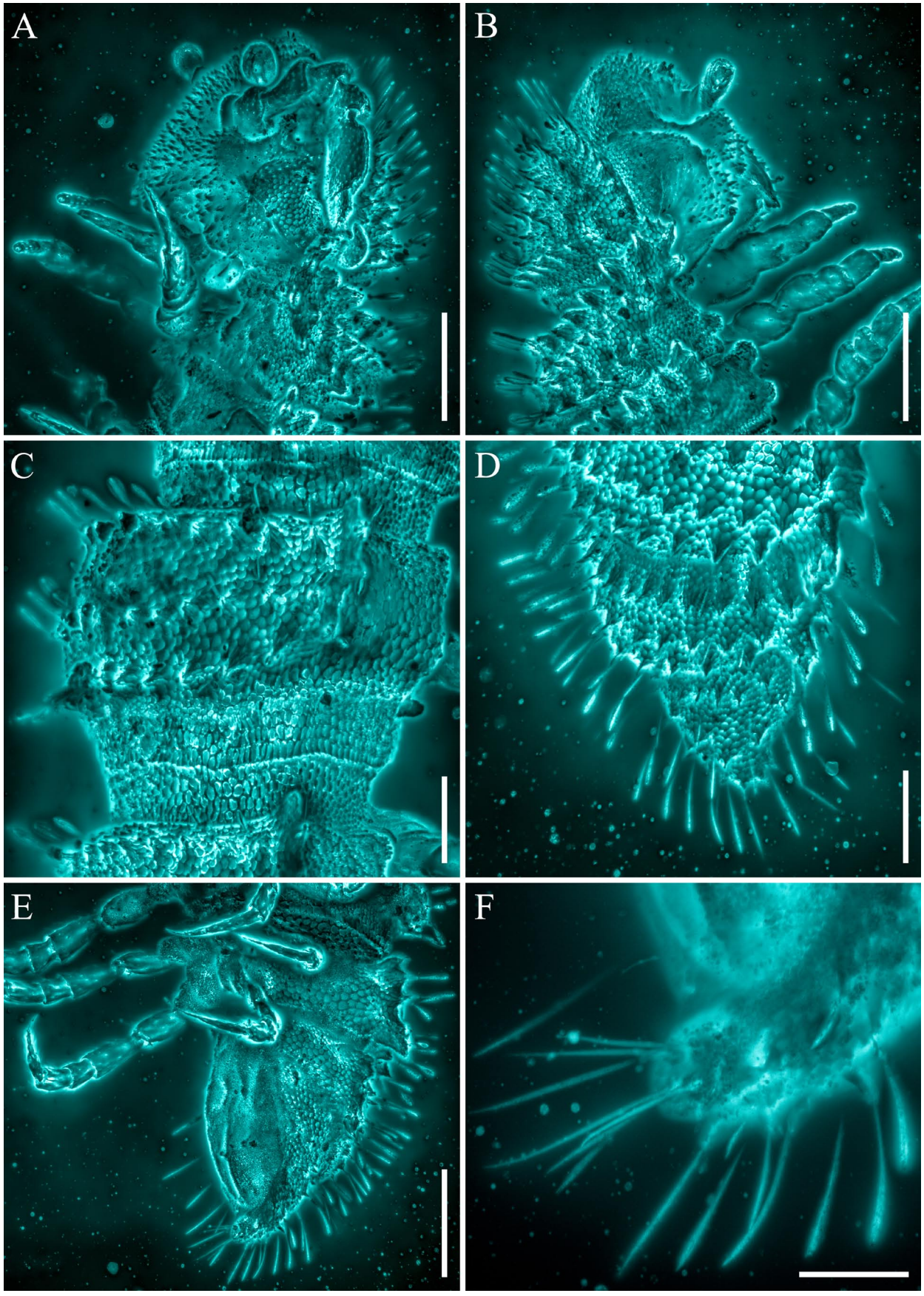

FIGURE 8. Adult female of *Monstrodesmus grimaldii* **sp. nov.**, paratype (NIGP175095), detail structures under CLSM. **A**, Ventrolateral view of the anterior body part. **B**, Dorsolateral view of the anterior body part. **C**, Detail structures of the 8th, 9th body-rings. **D**, Dorsolateral view of the posterior body part. **E**, Detail structures of the telson. **F**, Spinnerets on tip of epiproct. Scale bars = 200 μm in **A**, **B**, **D** and **E**, 100 μm in **C**, 50 μm in **F**.

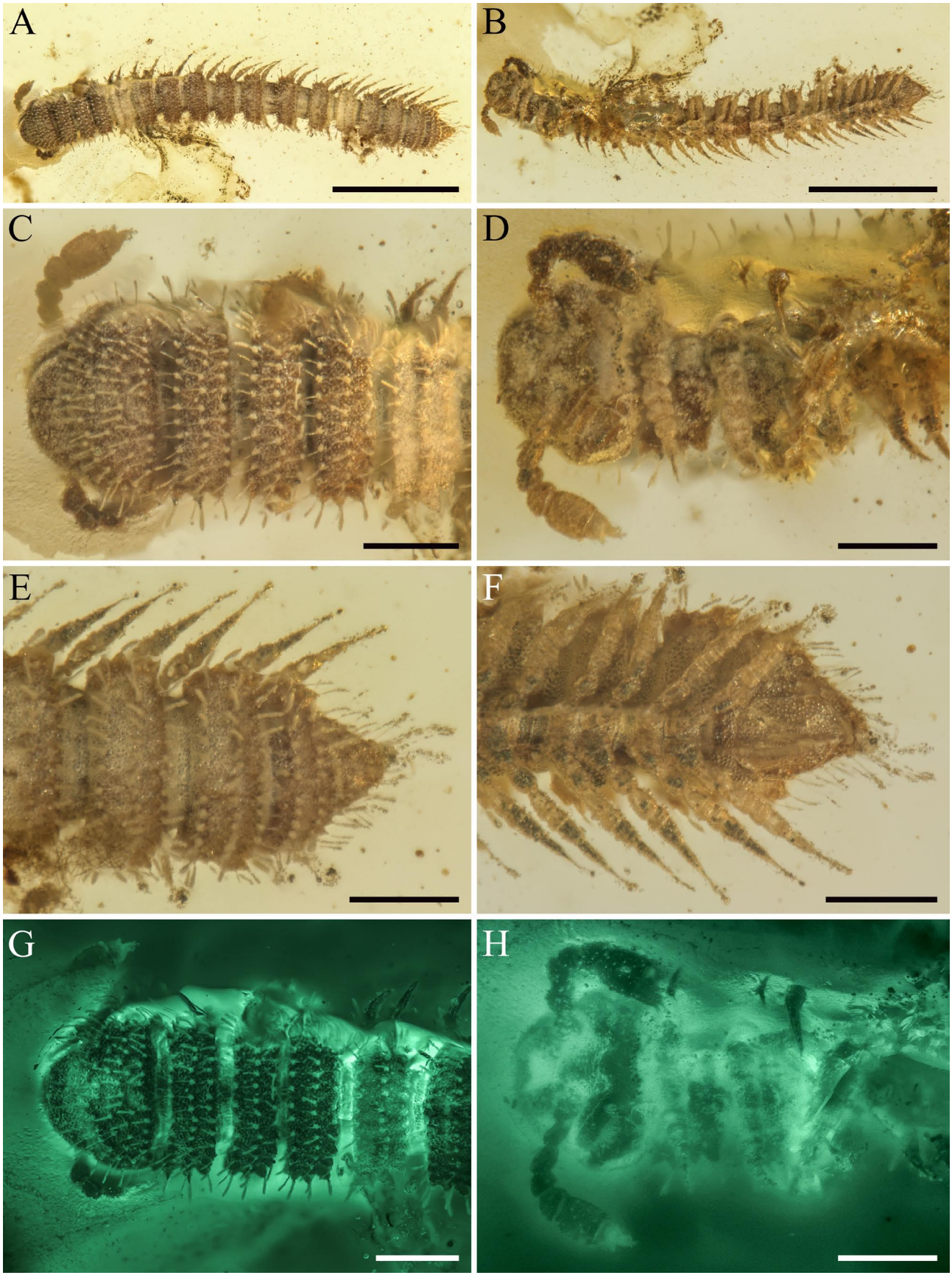

FIGURE 9. *Monstrodesmus grimaldii* **sp. nov.**, juvenile of 18 body-rings, male, paratype (NIGP175096). **A**, Dorsal view. **B**, Ventral view. **C**, **G**, Dorsal view of the anterior body part. **D**, **H**, Ventral view of the anterior body part. **E**, Dorsal view of the posterior body part. **F**, Ventral view of the posterior body part. **G** and **H** under green fluorescence. Scale bars = 0.5 mm in **A** and **B**, 0.2 mm in others.

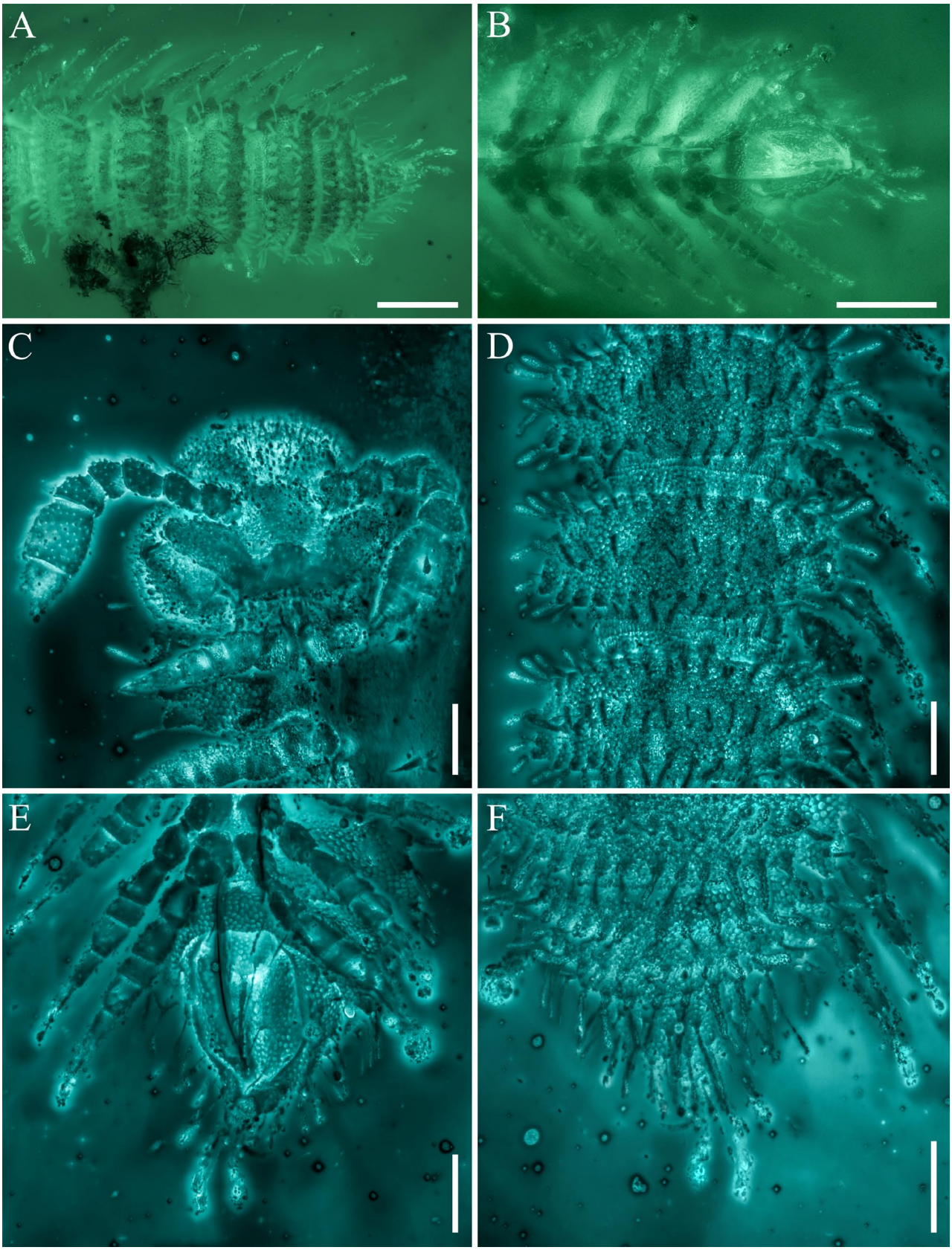

FIGURE 10. Detail structures of *Monstrodesmus grimaldii* **sp. nov.**, juvenile of 18 body-rings, male, paratype (NIGP175096). **A**, **F**, Dorsal view of the posterior body part. **B**, **E**,Ventral view of the posterior body part. **C**, Ventral view of head. **D**, Detail structures of the 8th to 10th body-rings. Scale bars = 0.2 mm in **A** and **B**, 0.1 mm in others.

formula normal, ozopores located on lateral-caudal corner of paraterga; legs short, without sphaerotrichomes; gonopod coxae large, subglobose, firmly attached to edges of gonopod aperture; telopodites elongate, fully exposed,

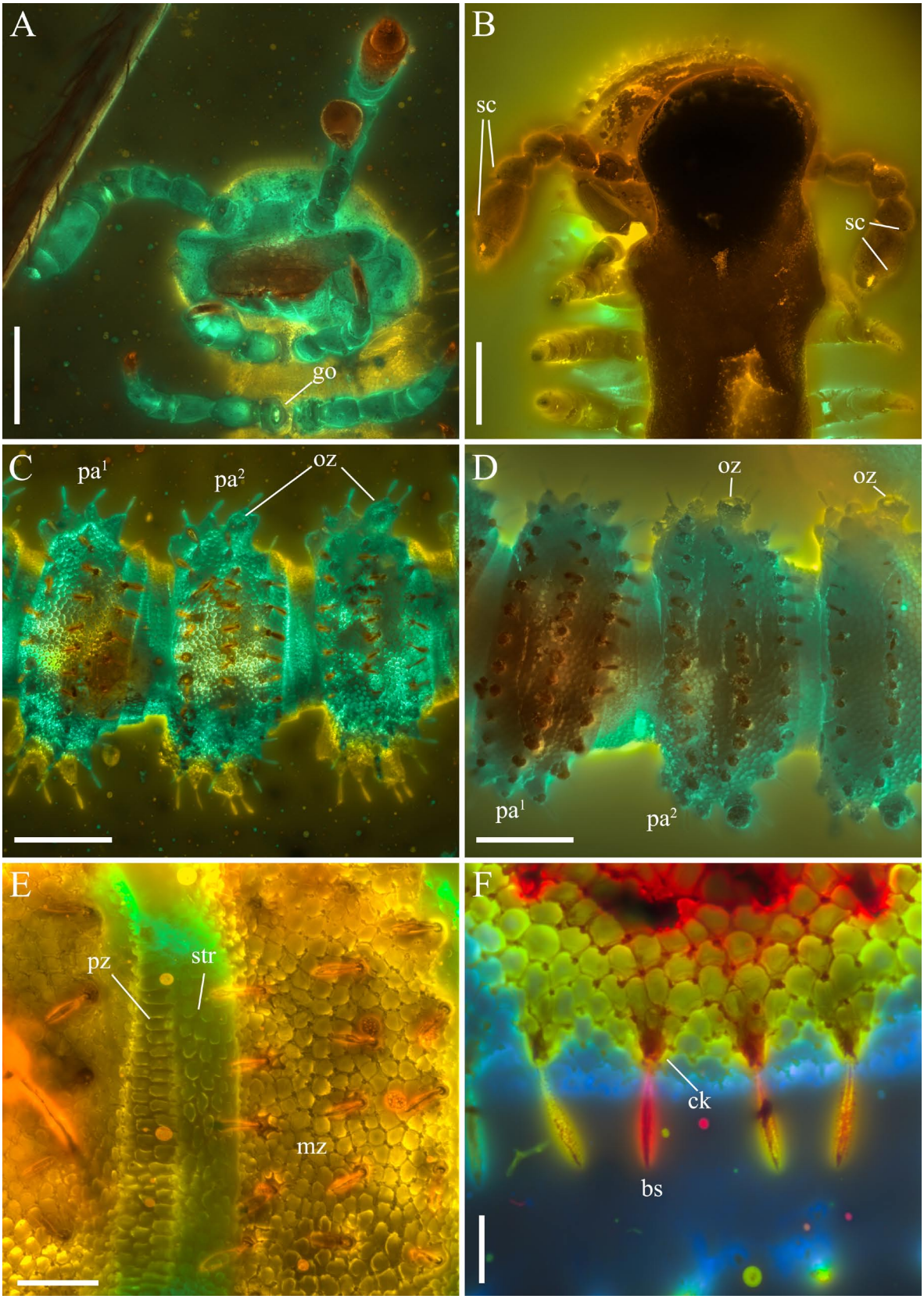

FIGURE 11. Head and tergal structures of adult male *Monstrodesmus grimaldii* **sp. nov.** under CLSM, with depth colour-coding. **A**, **C**, **E** and **F** NIGP175093; **B** and **D** NIGP175094. **A**, **B**, Ventral view of head. **C**, **D**, Detail structures of the 8th to 10th tergites. **E**, Detailed features of the 2nd to 3rd tergites. **F**, Setigerous knobs on the 18th metaterga. Abbreviations: go, gonapophyses; sc, bacilliform sensilla cluster; pa^1, paraterga without ozopores; pa^2, paraterga with ozopores; oz, ozopore; pz, prozonite; mz, metazonite; str, stricture between pro- and metazonite; ck, conic shape knob on metaterga; bs, basilliform seta inserted on knob. Scale bars = 50 μm in **E**, 10 μm in **F**, 200 μm in others.

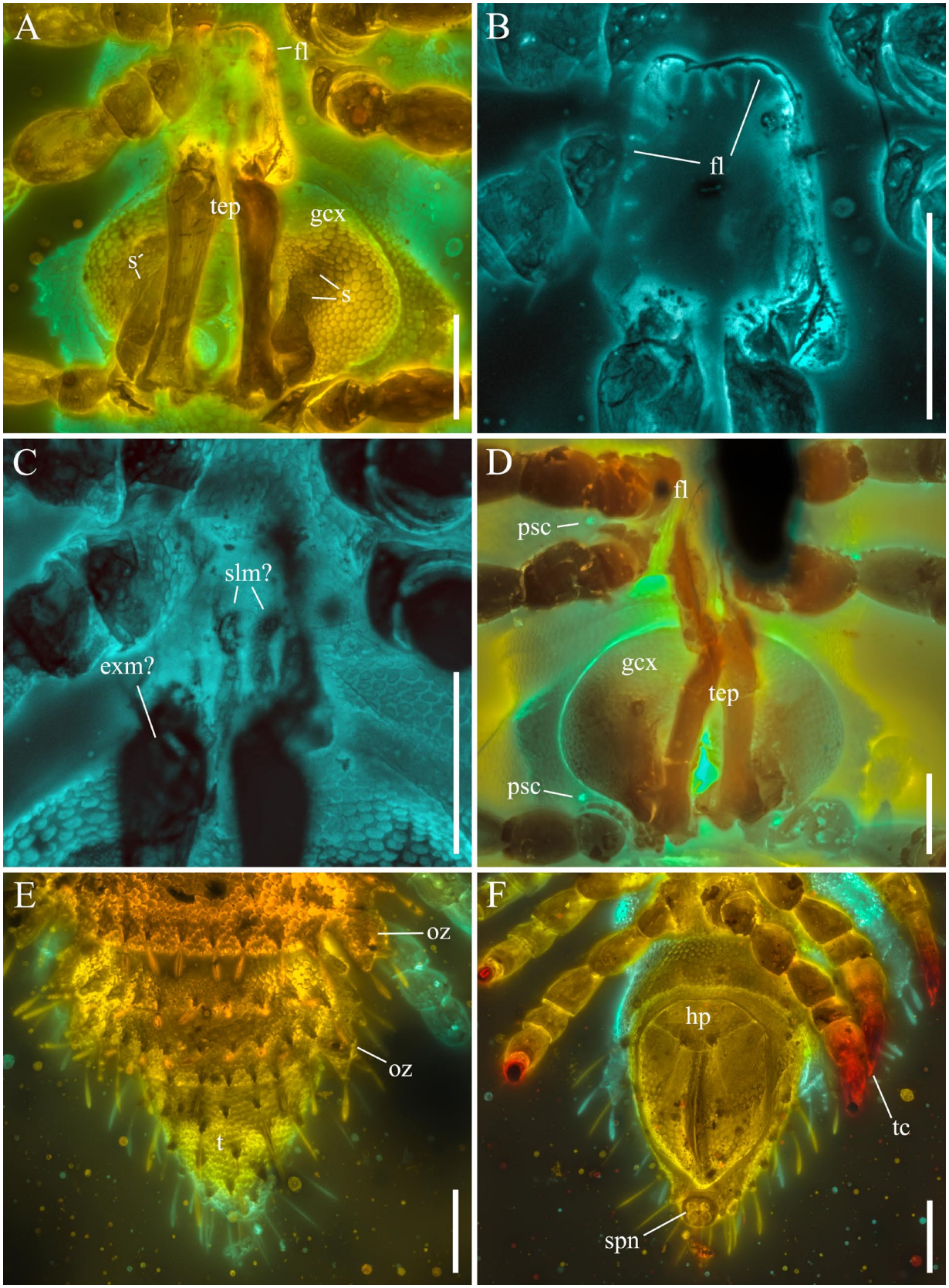

FIGURE 12. Gonopods and telson of adult male *Monstrodesmus grimaldii* **sp. nov.** under CLSM, **A**, **C**, **E** and **F** with depth colour-coding. **D**, NIGP175094; others NIGP175093. **A**, **D**, Ventral view of gonopods. **B**, Flagelliform branch of gonopod telopodite. **C**, Questionable solenomere of gonopod telopodite. **E**, Dorsal view of the posterior body part. **F**, Ventral view of telson. Abbreviations: gcx, gonopod coxa; tep, gonopod telopodite; s, seta on gonopod coxa; fl, flagelliform branch; slm?, questionable solenomere; exm?, questionable exomere; psc, pleurosternal carina; oz, ozopore; hp, hypoproct; spn, spinnerets; tc, tarsus claw. Scale bars = 50 μm in **B** and **C**, 100 μm in others.

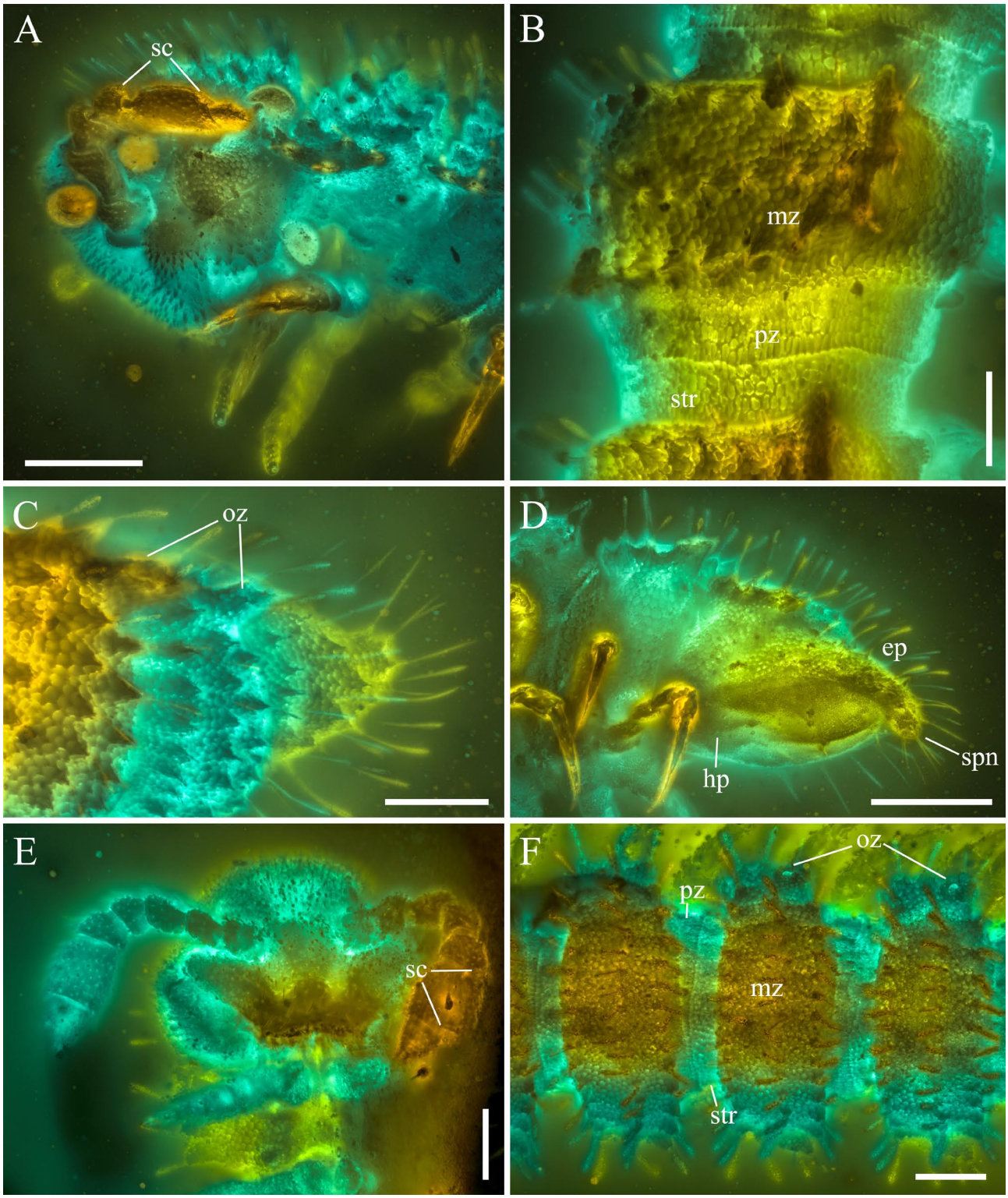

FIGURE 13. Detail structures of adult female and juvenile male *Monstrodesmus grimaldii* **sp. nov.** under CLSM, with depth colour-coding. **A**–**D** NIGP175094, adult female, **E** and **F** male juvenile of 18 body-rings. **A**, Lateral view of head. **B**, Dorsolateral view of of the 8th, 9th body-rings. **C**, Dorsolateral view of the posterior body part. **D**, Ventrolateral view of telson. **E**, Ventral view of head. **F**, Detail structures of the 8th to 10th body-rings. Abbreviations: sc, bacilliform sensilla cluster; pz, prozonite; mz, metazonite; str, stricture between pro- and metazonite; oz, ozopore; ep, epiproct; hp, hypoproct; spn, spinnerets. Scale bars = 0.1 mm.

most likely tripartite, held parallel to each other, with an unusual long flagelliform branch.

The new species differs from *Monstrodesmus flagellifer* in having 20 body rings in adult; stronger alveolate tegument; stronger projected knobs on insertion point of body setae; more setae on collum with different arrangement; more setae in number on each row of metaterga; wide and shallow strictures; slightly more

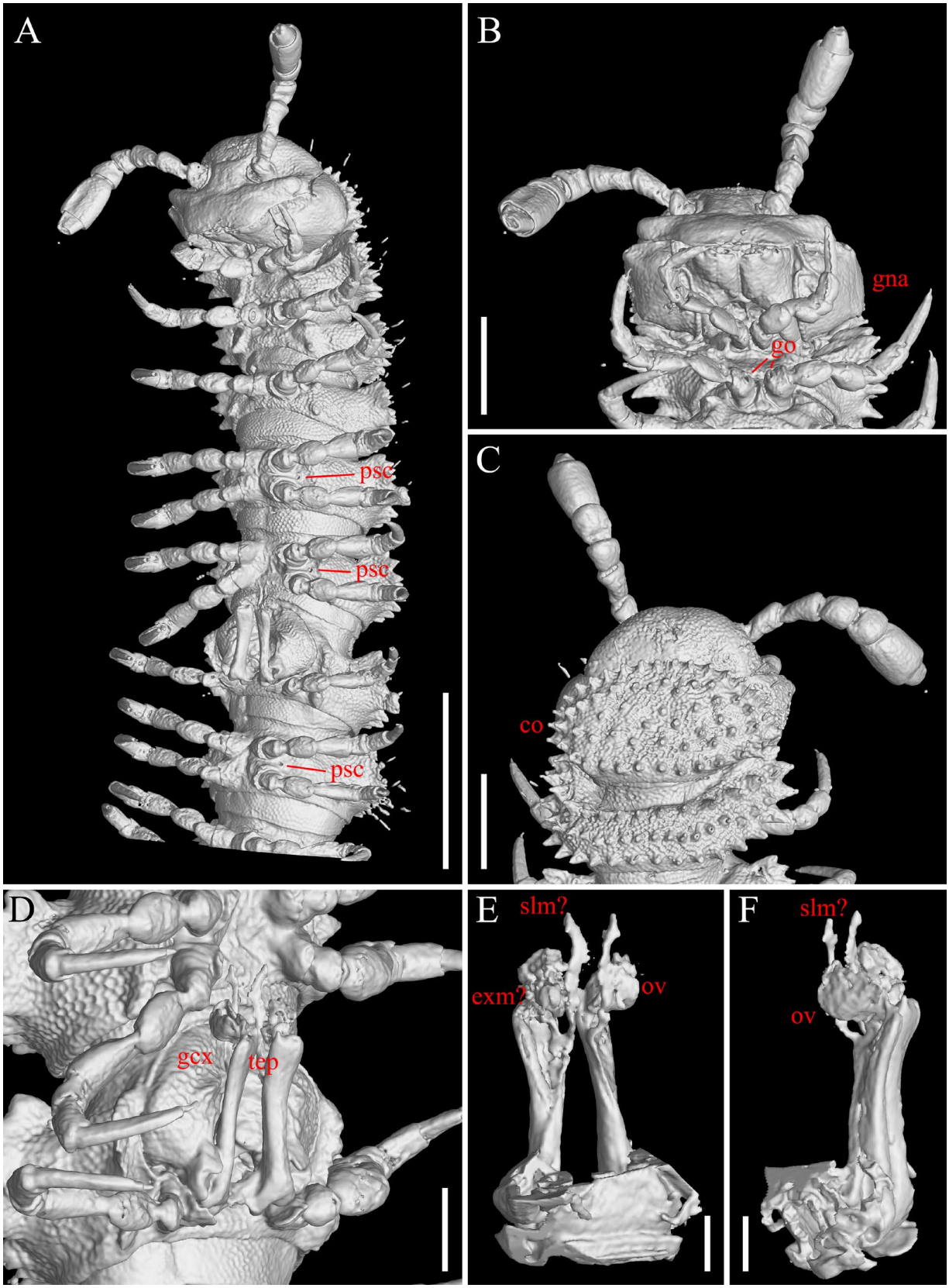

FIGURE 14. µCT reconstruction of the holotype of *Monstrodesmus grimaldii* **sp. nov. A**, Ventrolateral view of the anterior body part. **B**, Ventrocaudal view of head and the 1st leg-pair. **C**, Dorsal view of head, collum, the 2nd tergite. **D**, Ventrolateral view of gonopods. **E**, Dorsolateral view of gonopod telopodites. **F**, Lateral view of gonopod telopodites. Abbreviations: psc, pleurosternal carina; gna, gnathochilarium; go, gonapophyses; co, collum; gcx, gonopod coxa; tep, gonopod telopodite; slm?, questionable solenomere; exm?, questionable exomere; ov, oval shape structures on telopodite. Scale bars = 500 µm in **A**, 200 µm in **B** and **C**, 100 µm in **D**, 50 µm in **E** and **F**.

developed paraterga; pleurosternal carinae present; and flagelliform branch of gonopods relatively thinner with spines or palps along inner sides. By comparison, the sole living species of *Monstrodesmus* only has 19 body rings in the adult male (female unknown); only with 3 rows of 3+3 or 4+4 setae on collum and metaterga; stricture between pro- and metazonite deep and narrow; pleurosternal carinae absent; slightly stouter flagelliform branch of gonopods without spines or palps (Golovatch *et al.*, 2014). Although the number of body ring and the presence of pleurosternal carinae in the new species are different from the extant species of *Monstrodesmus*, and the tripartite feature of gonopod telopodites may slightly questionable in the new species (Fig. 14E, F), its overall gonopod features and the presence of the unique flagelliform branch still more similar to the extant species of *Monstrodesmus* rather than other known members. We considered that these differences may not enough for establishing a new genus, and therefore assign the new species to *Monstrodesmus*.

Given the characters and comparison discussed above, the new species from Burmese amber is similar to the extant trichopolydesmids in most characters, suggesting bradytely of Trichopolydesmidae from mid-Cretaceous to present day. The major evolution of the genus and the family may therefore be before the Cretaceous.

Acknowledgements

We sincerely thank two anonymous reviewers for valuable comments. Financial support was provided by the Second Tibetan Plateau Scientific Expedition and Research project (2019QZKK0706), the Strategic Priority Research Program of the Chinese Academy of Sciences (XDB26000000), the National Natural Science Foundation of China (42288201), and National Mineral Rock and Fossil Specimens Resource Center.

References

Azar, D., Perrichot, V., Néraudeau, D. & Nel, A. (2003) New psychodid flies from the Cretaceous ambers of Lebanon and France, with a discussion about *Eophlebotomus connectens* Cockerell, 1920 (Diptera, Psychodidae). *Annals of the Entomological Society of America*, 96, 117–127. https://doi.org/10.1603/0013-8746(2003)096[0117:NPFTCA]2.0.CO;2

Cruickshank, R.D. & Ko, K. (2003) Geology of an amber locality in the Hukawng Valley, northern Myanmar. *Journal of Asian Earth Sciences*, 21, 441–455. https://doi.org/10.1016/S1367-9120(02)00044-5

Enghoff, H., Golovatch, S.I., Short, M., Stoev, O. & Wesener, T. (2015) Diplopoda—taxonomic overview. *In*: Minelli, A. (Ed.), *Treatise on Zoology—Anatomy, taxonomy, biology. The Myriapoda.* Volume 2. Brill, Leiden and Boston, pp. 363–453. https://doi.org/10.1163/9789004188273_017

Fu, Y.Z., Li, Y.D., Su, Y.T., Cai, C.Y. & Huang, D.Y. (2021) Application of confocal laser scanning microscopy to the study of amber bioinclusions. *Palaeoentomology*, 4 (3), 266–278. https://doi.org/10.11646/palaeoentomology.4.3.14

Golovatch, S.I., Geoffroy, J.-J. & VandenSpiegel, D. (2014) Review of the millipede family Trichopolydesmidae in the Oriental realm (Diplopoda, Polydesmida), with descriptions of new genera and species. *ZooKeys*, 414, 19–65. https://doi.org/10.3897/zookeys.414.7671

Grimaldi, D.A., Engel, M.S. & Nascimbene, P.C. (2002) Fossiliferous Cretaceous amber from Myanmar (Burma): its rediscovery, biotic diversity, and paleontological significance. *American Museum Novitates*, 3361, 1–71. https://doi.org/10.1206/0003-0082(2002)361<0001:FCAFMB>2.0.CO;2

Mao, Y.Y., Liang, K., Su, Y.T., Li, J.G., Rao, X., Zhang, H., Xia, F.Y., Fu, Y.Z., Cai, C.Y. & Huang, D.Y. (2018) Various amberground marine animals on Burmese amber with discussions on its age. *Palaeoentomology*, 1 (1), 91–103. https://doi.org/10.11646/palaeoentomology.1.1.11

Ross, A.J. (2019) Burmese (Myanmar) amber checklist and bibliography 2018. *Palaeoentomology*, 2 (1), 22–84. https://doi.org/10.11646/palaeoentomology.2.1.5

Ross, A.J. (2021) Supplement to the Burmese (Myanmar) amber checklist and bibliography, 2020. *Palaeoentomology*, 4 (1), 57–76. https://doi.org/10.11646/palaeoentomology.4.1.11

Ross, A.J., Mellish, C., York, P. & Crighton, B. (2010) Burmese amber. *In*: Penney, D. (Ed.), *Biodiversity of fossils in amber from the major world deposits.* Siri Scientific Press, Manchester, pp. 208–235.

Shi, G.H., Grimaldi, D.A., Harlow, G.E., Wang, J., Wang, J., Yang, M.C., Lei, W.Y., Li, Q.L. & Li, X.H. (2012) Age constraint on Burmese amber based on U-Pb dating of zircons. *Cretaceous Research*, 37, 155–163. https://doi.org/10.1016/j.cretres.2012.03.014

Sierwald, P. & Spelda, J. (2021) MilliBase. Trichopolydesmidae Verhoeff, 1910. Available from: http://www.millibase.org/aphia.php?p=taxdetails&id=888798 (Accessed 2022-11-30)

Wesener, T. & Moritz, L. (2018) Checklist of the Myriapoda in Cretaceous Burmese amber and a correction of the Myriapoda identified by Zhang (2017). *Check List,* 14 (6), 1131–1140. https://doi.org/10.15560/14.6.1131

Zherikhin, V.V. & Ross, A.J. (2000) A review of the history, geology and age of Burmese amber (Burmite). *Bulletin of the Natural History Museum, London (Geology)*, 56, 3–10.